ISSN 1070-3284, Russian Journal of Coordination Chemistry, 2020, Vol. 46, No. 12, pp. 838–849. © Pleiades Publishing, Ltd., 2020.
Russian Text © The Author(s), 2020, published in Koordinatsionnaya Khimiya, 2020, Vol. 46, No. 12, pp. 758–769.

Coordination Compounds of Copper(II) with Schiff Bases Based on Aromatic Carbonyl Compounds and Hydrazides of Carboxylic Acids: Synthesis, Structures, and Properties

O. Danilescu[a], I. Bulhac[a], S. Shova[b], G. Novitchi[c], and P. Bourosh[d, *]

[a] *Institute of Chemistry, Chisinau, Republic of Moldova*
[b] *Petru Poni Institute of Macromolecular Chemistry, Iași, Romania*
[c] *French National Centre for Scientific Research, Grenoble, France*
[d] *Institute of Applied Physics, Chisinau, Republic of Moldova*
**e-mail: bourosh.xray@phys.asm.md*

Received January 2, 2020; revised February 28, 2020; accepted March 25, 2020

Abstract—The results of the synthesis and spectral (IR) and structural (X-ray diffraction analysis) studies are presented for five binuclear and one tetranuclear copper(II) complexes: $[Cu_2(H_2L^1)_2](SO_4)_2 \cdot 4H_2O$ (**I**), $[Cu_2(L^1)_2] \cdot 2MeOH \cdot 0.5EtOH$ (**II**), $[Cu_2(L^1)_2] \cdot 1.2EtOH \cdot 5.4H_2O$ (**III**), $[Cu_2(L^2)_2] \cdot H_2O$ (**IV**), $[Cu_2(L^2)_2] \cdot 0.1H_2O$ (**V**), and $[Cu_4(HL^2)_4(OH)_2](NO_3)_2 \cdot 6.75H_2O$ (**VI**), where H_2L^1 is 2,6-diacetylpyridine bis(isonicotinoylhydrazone) and H_2L^2 is 2,6-diacetylpyridine bis(nicotinoylhydrazone) (CIF files CCDC nos. 1967853 (**I**), 1967858 (**II**), 1967854 (**III**), 1967855 (**IV**), 1967856 (**V**), and 1967857 (**VI**)). In binuclear complexes **I–V** with the double spiral structure, both ligands are coordinated via the chelate-bridging mode (3 + 3) to different metal atoms, and the coordination polyhedron of the central atoms (distorted tetragonal bipyramid) is formed by the donor atoms N_4O_2. In tetranuclear complex cation **VI**, four copper atoms are joined by four tetradentate monodeprotonated ligands $(HL^2)^-$ and two bridging OH^- groups. Each metal atom in complex **VI** is characterized by the tetragonal pyramidal coordination in which the organic ligand is coordinated via the tridentate mode to one metal atom and via the monodentate mode to another atom involving the terminal nitrogen heteroatom (3 + 1).

Keywords: copper(II) complexes, polydentate Schiff bases, solvatomorph, X-ray diffraction analysis, IR spectra, magnetism

DOI: 10.1134/S1070328420090018

INTRODUCTION

The derivatives of 2,6-diacetylpyridine are of interest due to the diverse and pronounced biological activity [1, 2] and high complexation ability [3–7]. In particular, 2,6-diacetylpyridine bis(isonicotinoylhydrazone) (H_2L^1) and 2,6-diacetylpyridine bis(nicotinoylhydrazone) (H_2L^2) have nine donor atoms capable of involving in the formation of coordination bonds with metals, seven of them being nitrogen atoms and two of them being oxygen atoms. These ligands can exist in compounds in various tautomeric forms with various degrees of deprotonation (Scheme 1).

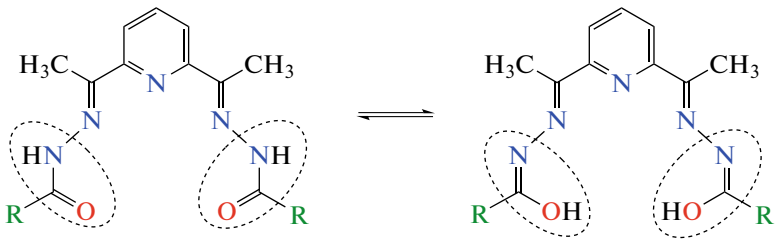

Scheme 1.

The syntheses and structural studies of the Co(II), V(II), V(IV), and Fe(III) complexes with the products of condensation of 2,6-diacetylpyridine with hydrazides of iso- and nicotinic acids were presented in our

previous works [8–10]. In this work, we present the results of synthesis and spectral (IR) and structural (X-ray diffraction analysis (XRD)) studies of six new Cu(II) complexes (five binuclear and one tetranuclear): $[Cu_2(H_2L^1)_2](SO_4)_2 \cdot 4H_2O$ (**I**), $[Cu_2(L^1)_2] \cdot 2MeOH \cdot 0.5EtOH$ (**II**), $[Cu_2(L^1)_2] \cdot 1.2EtOH \cdot 5.4H_2O$ (**III**), $[Cu_2(L^2)_2] \cdot H_2O$ (**IV**), $[Cu_2(L^2)_2] \cdot 0.1H_2O$ (**V**), and $[Cu_4(HL^2)_4(OH)_2](NO_3)_2 \cdot 6.75H_2O$ (**VI**), where H_2L^1 is 2,6-diacetylpyridine bis(isonicotinoylhydrazone) and H_2L^2 is 2,6-diacetylpyridine bis(nicotinoylhydrazone). Compounds **I** and **VI** are ionic, since their organic ligands are coordinated to the metal in the monodeprotonated form, and others are molecular complexes in which the organic ligands are doubly deprotonated.

EXPERIMENTAL

Commercial reagents and solvents (reagent grade) were used as received, and H_2L^1 and H_2L^2 were synthesized using known procedures [11, 12].

Synthesis of $[Cu_2(H_2L^1)_2](SO_4)_2 \cdot 4H_2O$ (I). Copper sulfate $CuSO_4 \cdot 5H_2O$ (0.25 g, 1.00 mmol) was dissolved in an ethanol–water (1 : 1.22 vol/vol) mixture (20 mL) to obtain solution 1. 2,6-Diacetylpyridine (0.16 g, 1.00 mmol) was dissolved in methanol (10 mL) to form solution 2. The dissolution of isonicotinic acid hydrazide (0.28 g, 2 mmol) in methanol (12 mL) gave solution 3. Solutions 2 and 3 were simultaneously added with permanent stirring to solution 1. The green-brown reaction mixture was heated at 60°C with a reflux condenser for 4 h, after which the solution was filtered and left to stay at room temperature in air for crystallization. Dark brown crystals of complex **I** suitable for XRD were formed after 24 h. The crystals were soluble in water, methanol, ethanol, and dimethylformamide (DMF) and insoluble in diethyl ether. The yield was 21.6% (based on copper(II) sulfate pentahydrate)).

For $C_{42}H_{46}N_{14}O_{16}S_2Cu_2$

Anal. calcd., %	C, 42.24	H, 3.88	N, 16.42	Cu, 10.64
Found, %	C, 42.11	H, 3.73	N, 16.30	Cu, 10.75

IR (ν, cm^{-1}): 3400 w, 3228 w, 2548 w, 1657 w, 1636 w, 1593 w, 1538 m, 1486 s, 1461 w, 1416 w, 1360 s, 1298 w, 1222 w, 1150 s, 1096 m, 1037 vs, 972 w, 929 w, 901 w, 843 m, 812 m, 753 m, 711 w, 686 m, 646 w, 608 s, 552 w, 519 w, 493 w, 452 w, 426 w.

Synthesis of $[Cu_2(L^1)_2] \cdot 2MeOH \cdot 0.5EtOH$ (II) and $[Cu_2(L^1)_2] \cdot 1.2EtOH \cdot 5.4H_2O$ (III). Copper sulfate $CuSO_4 \cdot 5H_2O$ (0.05 g, 0.2 mmol) and H_2L^1 (0.08 g, 0.2 mmol) were suspended in a DMF–methanol–ethanol (1 : 1.5 : 1.5 vol/vol/vol) mixture (8 mL). The syntheses was carried out in autoclaves with Teflon bushes (10 mL) under elevated pressure. The reaction mixture was heated to 80°C and kept for 48 h. A brown precipitate was filtered off and washed with a minor amount of a DMF–methanol–ethanol mixture, and the mother liquor was left to stay for crystallization in air. Dark brown crystals suitable for XRD were formed after 24 h. The crystals were insoluble in methanol, ethanol, DMF, and diethyl ether.

IR (ν, cm^{-1}): 3414 w, 3065 w, 2930 w, 1657 m, 1602 w, 1566 w, 1486 vs, 1457 m, 1412 w, 1370 vs, 1360 vs, 1314 m, 1296 w, 1260 w, 1224 w, 1160 m, 1134 w, 1097 w, 1056 s, 1012 m, 930 w, 914 w, 851 m, 838 w, 817 m, 759 m, 670 s, 668 w, 530 w, 583 w, 491 w, 437 w, 406 w.

Synthesis of $[Cu_2(L^2)_2] \cdot H_2O$ (IV) and $[Cu_2(L^2)_2] \cdot 0.1H_2O$ (V). Copper sulfate $CuSO_4 \cdot 5H_2O$ (0.05 g, 0.2 mmol) and H_2L^2 (0.08 g, 0.2 mmol) were suspended in a DMF–methanol–ethanol (1 : 1.5 : 1.5 vol/vol/vol) mixture (8 mL). The syntheses was carried out in autoclaves with Teflon bushes (10 mL) under elevated pressure. The reaction mixture was heated to 80°C and kept for 48 h. A brown precipitate was filtered off and washed with a minor amount of a DMF–methanol–ethanol mixture, and the filtrate was left for crystallization in air. Dark brown crystals suitable for XRD were formed in the filtrate after 24 h. The crystals were insoluble in methanol, ethanol, DMF, and diethyl ether.

IR (ν, cm^{-1}): 3382 w, 3075 w, 2336 w, 2053 w, 1655 m, 1580 m, 1558 w, 1495 s, 1460 m, 1409 w, 1369 vs, 1316 m, 1260 w, 1193 w, 1162 m, 1094 m, 1052 m, 1031 m, 927 w, 910 w, 814 m, 737 m, 715 w, 699 m, 672 w, 638 m, 618 m, 603 m, 501 w, 486 w, 459 w, 430 w, 405 w.

Synthesis of $[Cu_4(HL^2)_4(OH)_2](NO_3)_2 \cdot 6.75H_2O$ (VI). Copper nitrate $Cu(NO_3)_2 \cdot 3H_2O$ (0.06 g, 0.25 mmol) was dissolved in an ethanol–water (1 : 1.25 vol/vol) mixture (20 mL) to form solution 1. 2,6-Diacetylpyridine (0.04 g, 0.25 mmol) was dissolved in methanol (4 mL) (solution 2), and nicotinic acid hydrazide (0.07 g, 0.5 mmol) was dissolved in methanol (10 mL) (solution 3). Solutions 2 and 3 were simultaneously added with permanent stirring to solution 1. The mixture was refluxed with continuous stirring using a reflux condenser for 4 h, after which the solution was filtered and left to stay in air at room temperature for crystallization. Dark brown crystals suitable for XRD precipitated from the solution after 4 days. The crystals were soluble in water, methanol, ethanol, and DMF and insoluble in diethyl ether. The yield was 4% (based on copper(II) nitrate trihydrate).

For $C_{84}H_{87.50}N_{30}O_{22.75}Cu_4$

Anal. calcd., %	C, 47.15	H, 4.14	N, 19.64	Cu, 11.88
Found, %	C, 47.20	H, 4.16	N, 19.20	Cu, 11.75

IR (ν, cm^{-1}): 3380 w, 3248 w, 1751 w, 1667 m, 1629 w, 1610 w, 1596 w, 1560 w, 1534 m, 1507 m, 1474 w,

1369 vs, 1323 vs, 1297 vs, 1260 m, 1201 w, 1164 m, 1147 m, 1130 m, 1164 m, 1032 w, 1007 w, 992 w, 925 w, 909 w, 822 m, 748 w, 732 m, 699 m, 677 w, 620 w, 573 w, 540 w, 509 w, 482 w, 469 w, 452 w, 440 w, 407 w.

X-ray diffraction analysis. Experimental data for complexes **I**–**VI** were obtained at room temperature on an Xcalibur E diffractometer (graphite monochromator, MoK_α radiation). The unit cell parameters were determined and experimental data were processed using the CrysAlis Oxford Diffraction Ltd. program [13]. The structures of the compounds were determined by direct methods and refined by least squares in the anisotropic full-matrix variant for non-hydrogen atoms using the SHELX-97 program [14]. The positions of the hydrogen atoms of the water molecules were revealed from the difference Fourier syntheses, and positions of other hydrogen atoms were calculated geometrically and refined isotropically in the rigid body model with $U_{eff} = 1.2\ U_{equiv}$ or $1.5\ U_{equiv}$ of the corresponding O, N, and C atoms. An attempt to prepare compound **IV** as single crystals failed, and the experimental data were obtained from the twin, which was not separated and, hence, the *R* factor was not decreased. The crystallographic data and experimental characteristics for the structures of compounds **I**–**VI** are presented in Table 1. Selected interatomic distances and bond angles of the compounds are given in Table 2. The geometric parameters of intra- and intermolecular hydrogen bonds are listed in Table 3.

The positional and thermal parameters for the structures of complexes **I**–**VI** were deposited with the Cambridge Crystallographic Data Centre (CIF files CCDC nos. 1967853 (**I**), 1967858 (**II**), 1967854 (**III**), 1967855 (**IV**), 1967856 (**V**), 1967857 (**VI**); deposit@ccdc.cam.ac.uk or http://www.ccdc.cam.ac.uk).

RESULTS AND DISCUSSION

The broad absorption bands of medium and weak intensity observed in the ranges 2500–2325 and 2200–1800 cm^{-1} of the IR spectrum of compound **I** are possibly related to the migration of protons from N(2) and N(2)* to the heterocyclic nitrogen atoms (N(1) and N(1)*) of the terminal pyridine rings and to the formation of the PyH^+ fragments [15, 16]. The shift of the absorption band ν(C=O) + ν(CN) in the spectra of compounds **I**–**V** to the long-wavelength range to 1657 and 1636 cm^{-1} indicates the involvement of the carbonyl group in the coordination to the metal [8] and thus the stabilization of the organic ligands in the ketone form [17]. In the IR spectra of compounds **II**–**V**, the absorption bands of medium and high intensity at 1457 and 1360 cm^{-1} (complexes **II** and **III**) and at 1460 and 1369 cm^{-1} (compounds **IV** and **V**) correspond to bending vibrations of the CH_3 groups ($\delta_{asym}(CH_3)$ and $\delta_{sym}(CH_3)$, respectively) [16]. The IR spectra of complexes **II** and **III** exhibit absorption bands that can be assigned to the out-of-plane vibrations δ(C–H) of the aromatic rings: the absorption bands at 759 cm^{-1} for three adjacent hydrogen atoms (substitution type 1,3) and at 817 cm^{-1} for two adjacent hydrogen atoms (substitution type 1,4) [17, 18]. In the IR spectra of complexes **IV** and **V**, the out-of-plane vibrations δ(C–H) for three adjacent hydrogen atoms appear at 737 cm^{-1}, whereas those for the isolated hydrogen atom are observed at 814 cm^{-1} [17, 18].

The IR spectrum of complex **VI** exhibits the following significant absorption bands: at 3380 cm^{-1} corresponding to stretching vibrations (ν(OH) + ν(NH)), 1667 cm^{-1} caused by stretching vibrations of the carbonyl group (ν(C=O)), 1629 cm^{-1} caused by $\nu(C{=}N_{azometh.})$ and strong absorption in a range of 1260–1380 cm^{-1} caused by $\nu(NO_3^-)$ [16, 19], 1474 cm^{-1} caused by $\delta_{asym}(CH_3)$, and 1368 cm^{-1} caused by $\delta_{sym}(CH_3)$ [16]. The IR spectrum of the tetranuclear complex (**VI**) exhibits absorption bands at 732 and 822 cm^{-1} attributed to δ(C–H) of the aromatic rings for the substitution 1,3- and 1,4-types, respectively [17, 18].

Both molecular copper(II) complexes (**II**–**V**) and complexes of the ionic type (**I** and **VI**) were synthesized using various synthesis methods. The bis(deprotonated) organic ligands $(L^1)^{2-}$ or $(L^2)^{2-}$ are coordinated to the metal atom in compounds **II**–**V**, the neutral organic ligands H_2L^1 are coordinated to the metal atom in compound **I**, and the monodeprotonated ligands $(HL^2)^-$ are coordinated to the metal atom in complex **VI**. In the ionic compounds (**I** and **VI**), the charges of the complex cations are compensated by the outer-sphere inorganic anions SO_4^{2-} or NO_3^-, respectively.

Compound **I** that crystallizes in the orthorhombic space group *Ccca* was synthesized by the reaction of H_2L^1 with copper(II) sulfate in an ethanol–water–methanol mixture (Table 1). The structure is ionic and consists of binuclear complex cations $[Cu_2(H_2L^1)_2]^{4+}$ with the D_2 symmetry (Fig. 1a), SO_4^{2-} anions disordered around the binary axis, and H_2O molecules of crystallization in the ratio 1 : 2 : 4, respectively. The complex cation has the structure of a double spiral (Fig. 1b) in which the neutral organic ligands H_2L^1 are coordinated via the hexadentate chelate-bridging mode to two metal atoms, and the central N(4) atom of the ligand is bridging. The symmetrical coordination polyhedron of the metal atoms is a distorted tetragonal bipyramid and is formed by a set of donor atoms N_4O_2. The interatomic distances Cu(1)–O(1), Cu(1)–N(3), and Cu(1)–N(4) are 2.033(4), 1.930(6), and 2.502(7) Å, respectively (Table 2). The Cu(1)···Cu(1)* distance in the binuclear cation is 3.239(3) Å. Each neutral ligand H_2L^1 coordinates to both metal atoms to form four five-membered metallocycles of two types (CuOCNN and CuNCCN), two

Table 1. Crystallographic data, experimental characteristics, and structure refinement parameters for compounds **I**–**VI**

Parameter	Value					
	I	**II**	**III**	**IV**	**V**	**VI**
Empirical formula	$C_{42}H_{46}N_{14}O_{16}S_2Cu_2$	$C_{45}H_{45}N_{14}O_{6.5}Cu_2$	$C_{44.4}H_{50.3}N_{14}O_{10.6}Cu_2$	$C_{42}H_{36}N_{14}O_5Cu_2$	$C_{42}H_{34.2}N_{14}O_{4.1}Cu_2$	$C_{84}H_{87.5}N_{30}O_{22.75}Cu_4$
FW	1194.13	1013.03	1076.77	943.93	927.72	2135.50
T	293	293	293	293	293	293
Crystal system	Orthorhombic	Monoclinic	Orthorhombic	Monoclinic	Triclinic	Monoclinic
Space group	*Ccca*	*C2/c*	*Pban*	*C2/c*	$P\bar{1}$	*C2/c*
a, Å	15.8155(15)	24.4341(12)	15.4326(12)	22.500(5)	14.0736(8)	30.8824(16)
b, Å	27.0863(16)	14.3518(5)	14.1841(9)	16.017(5)	14.7059(10)	17.1598(7)
c, Å	13.4684(9)	15.4733(7)	13.9323(8)	15.519(5)	22.6625(11)	22.3395(10)
α, deg	90	90	90	90	108.326(5)	90
β, deg	90	114.108(4)	90	133.53(2)	90.609(4)	116.861(6)
γ, deg	90	90	90	90	110.675(6)	90
V, Å^3	5769.6(8)	4952.8(4)	3049.7	4055(2)	4126.5(5)	10561.1(8)
Z	4	4	2	4	2	4
ρ_{calc}, g/cm^3	1.375	1.359	1.173	1.546	1.493	1.343
μ, mm^{-1}	0.883	0.920	0.756	1.115	1.093	0.874
F(000)	2456	2092	1115	1936	1900	4398
Crystal sizes, mm	0.15 × 0.12 × 0.06	0.42 × 0.32 × 0.06	0.50 × 0.20 × 0.08	0.44 × 0.22 × 0.1	0.4 × 0.1 × 0.04	0.2 × 0.15 × 0.05
θ range for data collection, deg	2.983–25.042	3.003–25.050	3.22–24.99	3.09–24.99	2.87–25.05	3.02–25.05
Index ranges	$-11 \le h \le 18$, $-17 \le k \le 32$, $-8 \le l \le 16$	$-18 \le h \le 29$, $-15 \le k \le 17$, $-18 \le l \le 13$	$-8 \le h \le 18$, $-16 \le k \le 11$, $-16 \le l \le 11$	$-26 \le h \le 26$, $-13 \le k \le 19$, $-18 \le l \le 18$	$-16 \le h \le 16$, $-16 \le k \le 17$, $-26 \le l \le 18$	$-27 \le h \le 36$, $-20 \le k \le 17$, $-26 \le l \le 17$
Collected/ independent reflections	5201/2340 ($R_{int} = 0.0685$)	8293/4361 ($R_{int} = 0.0271$)	6584/2689 ($R_{int} = 0.0334$)	10 601/3566 ($R_{int} = 0.1346$)	22450/14562 ($R_{int} = 0.0423$)	18589/9320 ($R_{int} = 0.0465$)
Completeness, %	91.3	99.4	99.4	99.6	99.5	99.6
Number of reflections with $I > 2\sigma(I)$	1040	3110	1824	1620	8026	4030
Number of refined parameters	200	312	190	291	1121	671
GOOF	1.001	1.001	1.007	1.000	1.002	1.005
R factors ($I > 2\sigma(I)$)	$R_1 = 0.0840$, $wR_2 = 0.1753$	$R_1 =0.0533$, $wR_2 = 0.1529$	$R_1 = 0.0722$, $wR_2 = 0.2508$	$R_1 = 0.1516$, $wR_2 = 0.3563$	$R_1 = 0.0664$, $wR_2 = 0.1063$	$R_1 = 0.0758$, $wR_2 = 0.2065$
R factors (for all data)	$R_1 = 0.1861$, $wR_2 = 0.2000$	$R_1 = 0.0807$, $wR_2 = 0.1697$	$R_1 = 0.1027$, $wR_2 = 0.2748$	$R_1 = 0.2514$, $wR_2 = 0.4295$	$R_1 = 0.1372$, $wR_2 = 0.1261$	$R_1 = 0.1475$, $wR_2 = 0.2235$
$\Delta\rho_{max}/\rho_{min}$, e Å^{-3}	0.442, –0.314	0.653, –0.336	0.636, –0.465	3.153, –1.715	0.948, –0.706	1.066, –0.382

Table 2. Interatomic distances and bond angles in the coordination polyhedra of the structures of compounds **I–VI**

Bond	*d*, Å									
	I	**II**	**III**	**IV**	**V**				**VI**	
					Cu(1)	Cu(2)	Cu(3)	Cu(4)	Cu(1)	Cu(2)
Cu(1)–O(1)	2.034(4)	1.996(3)	2.037(3)	2.006(9)	2.144(3)	2.133(3)	2.000(4)	1.996(3)		
Cu(1)–N(3)	1.929(6)	1.923(3)	1.934(4)	1.940(10)	1.962(4)	1.962(4)	1.922(4)	1.916(4)		
Cu(1)–N(4)	2.501(5)	2.350(3)	2.452(4)	2.213(9)	2.687(4)	2.709(4)	2.275(4)	2.328(5)	2.068(6)	2.071(7)
Cu(1)–O(2)*/O(2)		2.079(3)		2.109(9)	1.979(3)	1.985(4)	2.138(3)	2.060(3)	1.967(5)	1.987 (6)
Cu(1)–N(4)*/N(4)		2.576(3)		2.630(9)	2.179(4)	2.233(4)	2.642(4)	2.702(4)		
Cu(1)–N(5)*/N(5)		1.936(3)		1.994(9)	1.920(4)	1.923(4)	1.956(4)	1.959(4)	1.921(6)	1.915(6)
Cu(1)–N(1)*									1.991(6)	1.978(6)
Cu(1)–$O(1)_{OH}$									2.309(5)	2.304(5)
Angle	ω									
	I	**II**	**III**	**IV**	**V**				**VI**	
					Cu(1)	Cu(2)	Cu(3)	Cu(4)	Cu(1)	Cu(2)
O(1)Cu(1)O(1)*/O(2)*	118.1(3)	117.04(12)	117.7(2)	109.9(4)	108.59(15)	115.05(15)	113.02(14)	120.33(15)		
O(1)Cu(1)N(3)	79.6(2)	79.86(12)	79.63(15)	80.2(4)	77.79(15)	77.64(15)	77.91(15)	79.02(16)		
O(1)Cu(1)N(3)*/N(5)*	104.4(2)	101.57(11)	104.86(15)	97.2(4)	113.37(15)	112.20(15)	98.37(16)	97.93(16)		
O(1)Cu(1)N(4)	150.29(13)	152.87(10)	151.76(10)	157.1(4)	148.87(12)	147.81(12)	154.55(14)	150.96(14)		
O(1)Cu(1)N(4)*	78.29(16)	78.13(11)	79.33(13)	78.5(3)	88.10(15)	84.67(14)	76.87(14)	74.68(13)		
N(3)Cu(1)N(3)*/N(5)*	172.5(4)	170.90(12)	171.5(2)	169.8(4)	168.70(18)	170.12(17)	170.10(18)	170.19(17)		
N(3)Cu(1)N(4)	72.08(18)	75.13(11)	73.99(12)	78.8(4)	71.16(15)	71.03(15)	76.51(17)	74.89(17)		
N(3)Cu(1)N(4)*	102.88(18)	99.21(11)	100.14(12)	97.2(3)	104.77(17)	103.78(16)	98.72(15)	99.72(15)		
N(3)Cu(1)O(2)*		108.40(12)		111.5(4)	95.21(16)	97.11(15)	111.85(15)	110.34(17)		
N(4)Cu(1)N(4)*	99.3(2)	95.53(10)	95.40(18)	95.2(3)	94.51(14)	95.56(14)	98.08(14)	95.11(13)		
N(4)Cu(1)N(5)*/N(5)		101.53(11)		101.9(4)	97.74(15)	99.10(15)	103.63(16)	104.20(16)	81.3(2)	79.7(3)
N(4)Cu(1)O(2)*/O(2)		81.29(11)		86.4(4)	76.98(14)	76.76(14)	84.30(14)	82.67(15)	159.6(2)	160.2(2)
O(2)*Cu(1)N(4)*		150.20(10)		150.9(3)	156.41(14)	154.09(14)	148.93(12)	147.98(14)		
O(2)*/O(2)Cu(1)N(5)*/N(5)		79.10(11)		78.6(4)	79.83(17)	79.68(17)	79.62(17)	80.08(17)	78.5(2)	80.7(3)
N(4)*Cu(1)N(5)*		72.49(11)		72.6(3)	78.21(18)	77.14(18)	71.40(15)	70.54(14)		
N(1)*Cu(1)O(2)									92.8(2)	93.1(2)
N(1)*Cu(1)N(4)									105.4(2)	104.1(3)
N(1)*Cu(1)N(5)									159.5(2)	159.4(3)
N(1)*Cu(1)$O(1)_{OH}$									100.1(2)	101.2(2)
$O(1)_{OH}$Cu(1)O(2)									91.56(18)	87.37(19)
$O(1)_{OH}$Cu(1)N(4)									94.21(19)	98.7(2)
$O(1)_{OH}$Cu(1)N(5)									98.7(2)	98.2(2)

*__I__: $x + 0, -y + 1/2, -z + 1/2$; __II__: $-x + 2, y, -z + 1/2$; __III__: $x, -y + 1/2, -z + 2$; __IV__: $-x + 2, y, -z + 1/2$; __VI__: $-x + 2, y, -z + 1/2$.

Table 3. Geometric parameters of hydrogen bonds in compounds **I**–**VI**

D–H···A	Distance, Å			Angle DHA, deg	Symmetry transform for A
	D–H	H···A	D···A		
			I		
N(1)–H(1)···O(4)	0.86	1.76	2.59(1)	163	$-x + 1/2, -y + 1/2, -z + 1$
N(1)–H(1)···O(2)	0.86	1.88	2.69(1)	157	$x, y - 1/2, -z + 1$
N(1)–H(1)···O(5)	0.86	2.36	2.99(2)	130	$-x + 1/2, -y + 1/2, -z + 1$
O(1*w*)–H(1)···O(3*w*)	0.85	1.84	2.69(4)	172	$x, -y + 1, z + 1/2$
O(1*w*)–H(2)···O(2)	0.83	1.93	2.76(3)	175	x, y, z
O(1*w*)–H(2)···O(5)	0.83	2.65	3.26(3)	131	x, y, z
O(2*w*)–H(1)···O(2*w*)	0.81	2.03	2.81(6)	161	$-x + 1, y, -z + 1/2$
O(2*w*)–H(2)···O(5)	0.84	2.16	2.83(4)	137	x, y, z
O(2*w*)–H(2)···O(2)	0.84	2.23	3.03(3)	158	x, y, z
O(3*w*)–H(1)···O(1*w*)	0.84	1.89	2. 56(4)	137	$-x + 1, y, -z + 1/2$
O(3*w*)–H(1)···O(3*w*)	0.84	2.28	2.98(5)	142	$-x + 1, -y + 1, -z$
O(3*w*)–H(2)···O(5)	0.74	2.37	3.02(3)	149	x, y, z
O(4*w*)–H(1)···O(4*w*)	0.80	2.56	3.35(6)	175	$-x + 1, -y + 1, -z$
O(4*w*)–H(2)···O(3)	0.93	1.99	2.69(3)	131	x, y, z
			II		
O(1*M*)–H(1)···N(7)	0.82	2.12	2.934(7)	171	x, y, z
			III		
O(1*w*)–H(1)···N(1)	0.88	2.01	2.884(7)	176	x, y, z
O(1*w*)–H(2)···O(2*w*)	0.83	1.93	2.758(9)	175	x, y, z
O(2*w*)–H(1)···O(1*E*)	0.88	2.02	2.67(2)	130	x, y, z
O(2*w*)–H(2)···O(1*E*)	0.85	1.90	2.67(3)	149	$-x + 3/2, y, -z + 1$
O(1*E*)–H(1)···O(1*E*)	0.85	2.32	3.17(5)	178	$-x + 3/2, y, -z + 1$
			IV		
O(1*w*)–H(1)···O(1)	0.87	2.25	2.98(3)	141	$-x + 2, y, -z + 1/2$
O(1*w*)–H(1)···O(2)	0.87	2.10	2.52(2)	110	x, y, z
			V		
O(1*w*)–H(1)···O(1*B*)	0.90	2.37	3.27(3)	179	$x, y + 1, z$
O(1*w*)–H(2)···N(6*C*)	1.08	2.27	3.36(3)	176	x, y, z
			VI		
$O(1)_{OH}$–H(1)···O(1*B*)	0.73	2.15	2.710(6)	135	x, y, z
$O(1)_{OH}$–H(1)···O(1*A*)	0.73	2.39	2.836(7)	122	x, y, z
N(2*A*)–H···O(2)	0.86	2.50	3.154(1)	134	$-x + 2, y, -z + 1/2$
N(2*B*)–H···O(3)	0.86	2.37	3.220(1)	173	x, y, z
O(1*w*)–H(1)···N(7*B*)	0.86	2.05	2.911(2)	178	x, y, z
O(1*w*)–H(2)···O(3)	0.85	1.89	2.738(2)	178	$x + 1/2, y + 1/2, z$
O(2*w*)–H(1)···O(2*w*)	0.80	1.89	2.69(4)	175	x, y, z
O(2*w*)–H(2)···O(2*B*)	0.81	2.23	3.034(2)	169	x, y, z
O(3*w*)–H(1)···N(7*A*)	0.99	1.97	2.951(2)	176	x, y, z
O(4*w*)–H(1)···O(1*w*)	0.69	1.91	2.61(3)	179	$x, -y + 1, z - 1/2$
O(4*w*)–H(2)···O(6*w*)	0.89	2.06	2.95(4)	172	x, y, z
O(5*w*)–H(1)···O(7*w*)	0.85	2.37	3.07(3)	139	x, y, z
O(6*w*)–H(1)···O(9*w*)	0.90	2.19	2.86(3)	130	$x, -y + 1, z - 1/2$
O(7*w*)–H(1)···O(5*w*)	0.96	2.08	2.97(3)	154	x, y, z
O(8*w*)–H(1)···O(4*w*)	0.85	1.95	2.80(3)	180	x, y, z

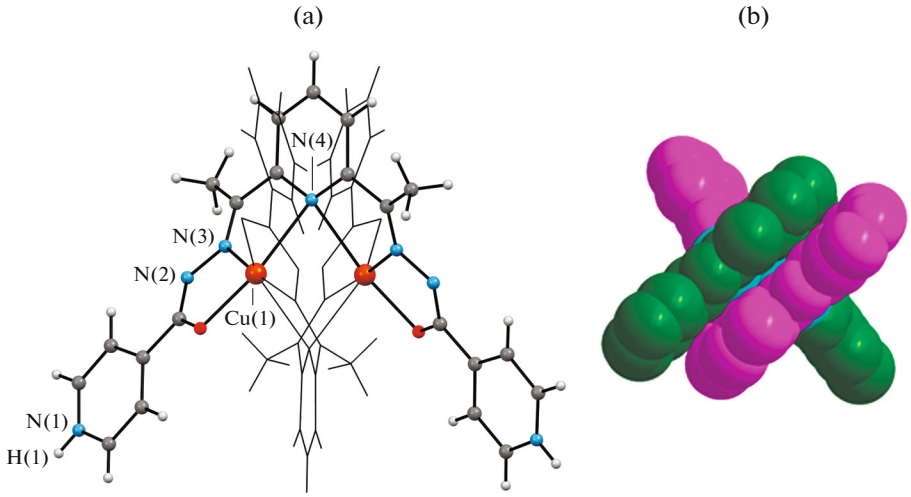

Fig. 1. Structure of the complex cation $[Cu_2(H_2L^1)_2]^{4+}$ with the partial notation of atoms: (a) the second ligand is drawn by thin lines for clarity and (b) the structure of the double spiral for the complex cation $[Cu_2(H_2L^1)_2]^{4+}$.

of which coordinate to one metal atom and two others coordinate to the second metal atom. A similar coordination mode of these ligands has previously been found in the binuclear Cu(II) [12, 20], Co(II) [21], Ni(II) [5, 22], and Zn(II) [23] complexes with ligands of this class. It was concluded on the basis of diverse steric concepts and an analysis of the Fourier syntheses that the hydrogen atom, which should be localized at the nitrogen atom of the hydrazine fragment in H_2L^1, is stabilized at the nitrogen atom of the terminal heterocycle (N(1)). It is known that the CNC angle in the pyridine fragments is sensitive to protonation [24, 25] and, hence, the CNC bond angle at the nitrogen atom in the terminal pyridine cycle in complex **I** is larger than 120° (∠CNC 122.1(7)°), which also confirms the proton transfer and formation of the PyH^+ fragment.

An analysis of the crystal structure shows that the complex cations and SO_4^{2-} anions are linked to each other into layers parallel to the *bc* plane by both intermolecular hydrogen bonds (IHB) N–H···O and weaker C–H···O bonds (Table 3, Fig. 2) and the water molecules are linked with the latter and between each other by IHB O(*w*)–H···O, O(*w*)–H···O(w), and C–H···O(*w*).

When the solvothermal synthesis method was used, the reactions of H_2L^1 or H_2L^2 with copper(II) sulfate afforded two solvatomorphs: $[Cu_2(L^1)_2] \cdot 2MeOH \cdot 0.5EtOH$ (**II**) and $[Cu_2(L^1)_2] \cdot 5.4H_2O \cdot 1.2EtOH$ (**III**) or $[Cu_2(L^2)_2] \cdot H_2O$ (**IV**) and $[Cu_2(L^2)_2] \cdot 0.1H_2O$ (**V**), respectively. Compounds **II**–**IV** crystallize in more symmetric space groups of the orthorhombic or monoclinic crystal system, whereas complex **V** crystallizes in the triclinic space group $P\bar{1}$ (Table 1). Two crystallographically independent nonsymmetric complexes are stabilized in the unit cell of the latter. The structures of the molecular complexes $[Cu_2(L^1)_2]$ and $[Cu_2(L^2)_2]$ in compounds **II**–**V** are similar to that found in complex cation **I** (Fig. 3). However, in these compounds, the organic ligands $(L^{1/2})^{2-}$ coordinate to the metal atom in the doubly deprotonated keto form. The coordination polyhedra of the metal atoms in compounds **II**–**V** are distorted tetragonal bipyramids and formed by the donor atoms N_4O_2 belonging to two different ligands. The interatomic distances Cu(1)–O(1)/O(2), Cu(1)–N(3)/N(5), and Cu(1)–N(4)/N4* are equal, on the average, to 2.106, 1.942, and 2.459 Å, respectively (Table 2). The Cu(1)···Cu(1)* distance in molecular complex **II** is 3.315(1) Å, that in compound **III** is 3.300(2), that in compound **IV** is 3.278(3), and

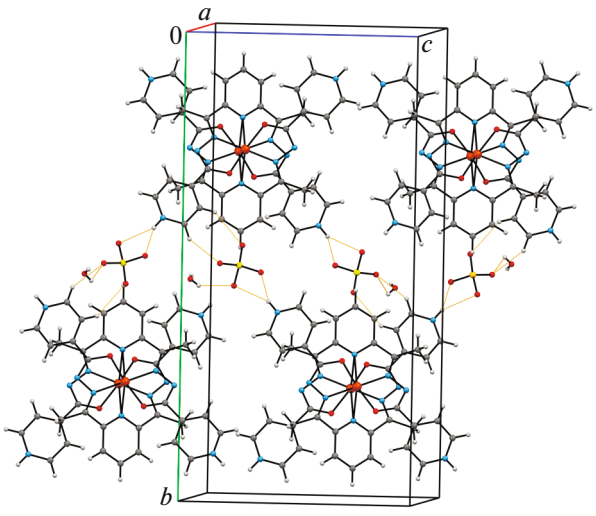

Fig. 2. Fragment of the crystal structure of complex **I**.

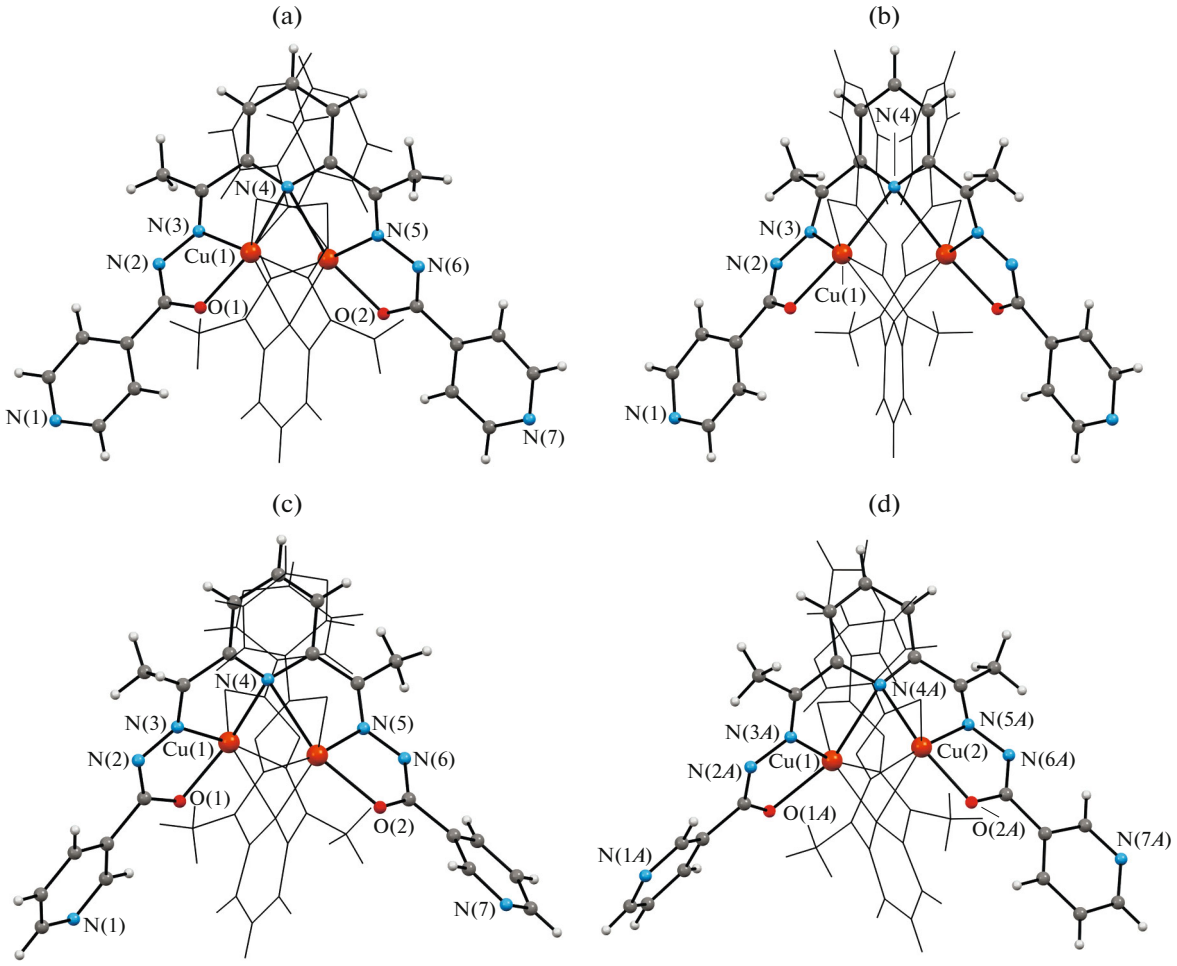

Fig. 3. Structures of the binuclear molecular complexes $[Cu_2(L^1)_2]$ in compounds (a) **II** and (b) **III**, (c) $[Cu_2(L^2)_2]$ in compound **IV**, and (d) one crystallographically independent complex in compound **V** with the partial notation of atoms.

the Cu(1)···Cu(2) and Cu(3)···Cu(4) distances in complex **V** are 3.280(1) and 3.318(1) Å, respectively.

An analysis of the crystal structures shows that in compound **II** the molecular complexes are linked with each other into chains via weak IHB C–H···N(1), the methanol molecules are joined with them by the O–H···N(7) bonds, whereas the ethanol molecules are arranged in cavities between them (Table 3, Fig. 4a). Both IHB O(*w*)–H···N between the water molecules and complexes and the IHB formed between the water molecules of crystallization and ethanol molecules (Fig. 4b) can be distinguished in compound **III**. The complexes in compound **IV** are bound to the water molecules by IHB O(*w*)–H···O and weak C–H···O(*w*) bonds (Fig. 4c). Weak IHB C–H···N(7)/N(7) and C–H···O(1)/O(2), which join the molecular complexes in the crystal, and weak IHB C–H···O(1)/N(6) and C–H···O(1*w*) linking the water residues with the complexes (Fig. 4d) can be distinguished in compound **V**.

Compound $[Cu_4(HL^2)_4(OH)_2](NO_3)_2 \cdot 6.75H_2O$ (**VI**), which crystallizes in the monoclinic space group *C*2/*c*, was synthesized from a $Cu(NO_3)_2 \cdot 3H_2O$–2,6-diacetylpyridine–nicotinic acid hydrazide system in a molar ratio of 1 : 1 : 2. The water molecules are localized in nine positions with various populations. The structure of the compound is ionic and consists of tetranuclear complex cations $[Cu_4(HL^2)_4(OH)_2]^{2+}$ with the C_2 symmetry (Fig. 5a), anions NO_3^-, and H_2O molecules of crystallization. In the complex cation, four copper(II) ions are linked by four monodeprotonated ligands $(HL^2)^-$, and two organic ligands coordinate to each metal atom, one of which coordinates by the donor atoms O(2)N(5)N(4) and another coordinates by the terminal N(1) atom of the pyridine heterocycle. These four atoms are arranged in the base of the square-pyramidal polyhedron of the metal, and the polyhedron is supplemented by the O atom of the bridging anion OH^-. The interatomic distances Cu(1)–O(2), Cu(1)–N(4), Cu(1)–N(5), Cu(1)–N(1), and Cu(1)–$O(1)_{OH}$ are equal, on the average, to 1.977, 2.069, 1.918, 1.985, and 2.306 Å, respectively (Table 2). As a result, $(HL^2)^-$ is a tetradentate chelate-

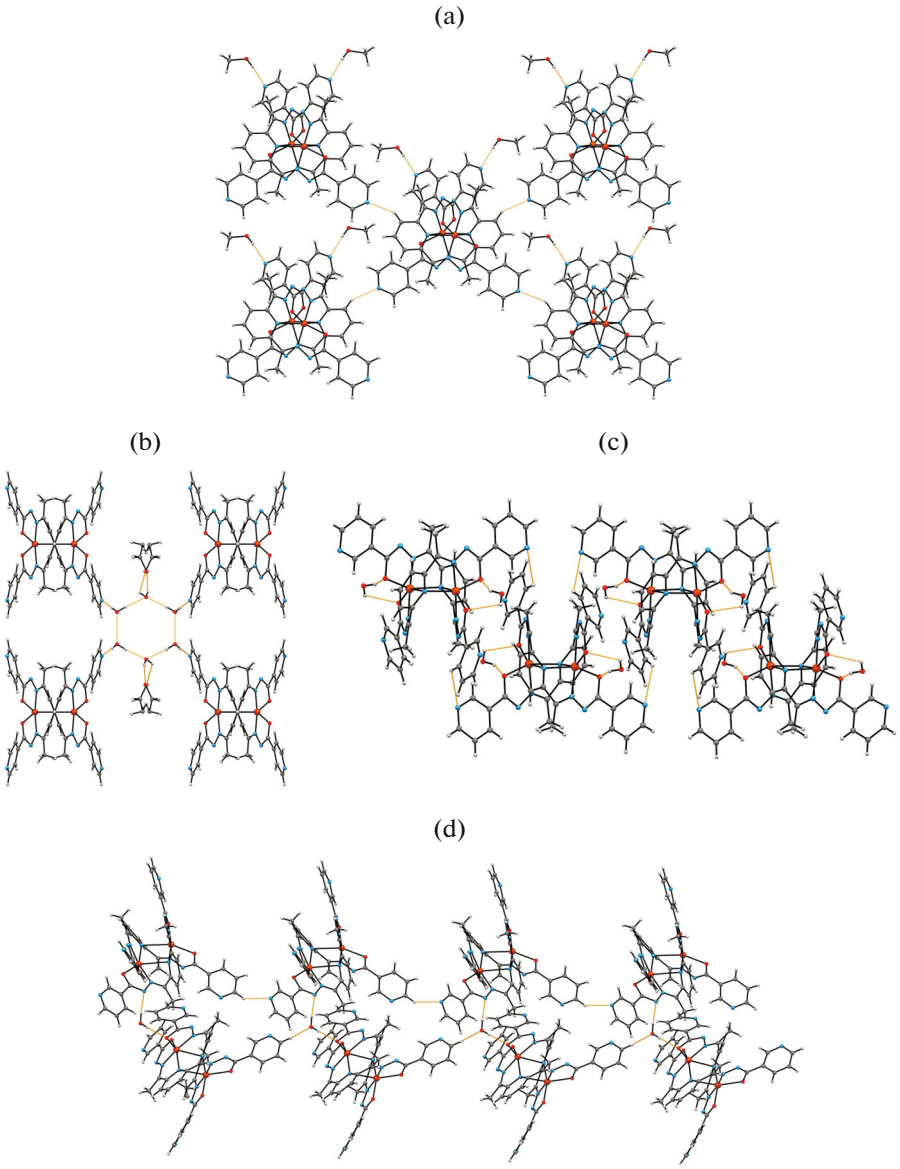

Fig. 4. Fragments of the crystal structures of compounds (a) **II**, (b) **III**, (c) **IV**, and (d) **V**.

bridging ligand, which coordinates via the tridentate mode to one metal atom by the set of donor atoms ONN to form two five-membered metallocycles via the mode found for compounds **I**–**V**, whereas the coordination to another metal atom occurs via the monodentate mode by one terminal N(1) atom of the heterocycle. Unlike the localized H atom at the terminal N atom of the heterocycle of the organic ligand found in compound **I**, another tautomeric form of the latter is stabilized in complex **VI** and the remained H atom is localized at the N atom of the azomethine group (N(2)) due to deprotonation. The Cu(1)···Cu(2) and Cu(1)···Cu(2)* distances in the cation are 4.298(4) and 9.092(1) Å, respectively.

An analysis of the complicated system of hydrogen bonds shows that the tetranuclear complex cation is stabilized by intramolecular hydrogen bonds $O(1)_{OH}$–H···O(1*A*)/O(1*B*) (Table 3) and the complex cations and NO_3^- anions are bound to each other into layers by the IHB O(*w*)–H···O and O(*w*)–H···N (Table 3, Fig. 6) and weaker C–H···O bonds both between the cations and between the cations and anions. Other water molecules are mainly joined between each other by IHB O(*w*)–H···O(*w*) and are linked to the main framework of the structure by O(*w*)–H···O/N and C–H···O(*w*).

In the binuclear Cu(II) complexes, the coordinating agents H_2L^1 and H_2L^2 act as bridging ligands, and a magnetic interaction between the copper atoms cannot be excluded. The manifestation of the magnetic interaction, namely, antiferromagnetic interaction,

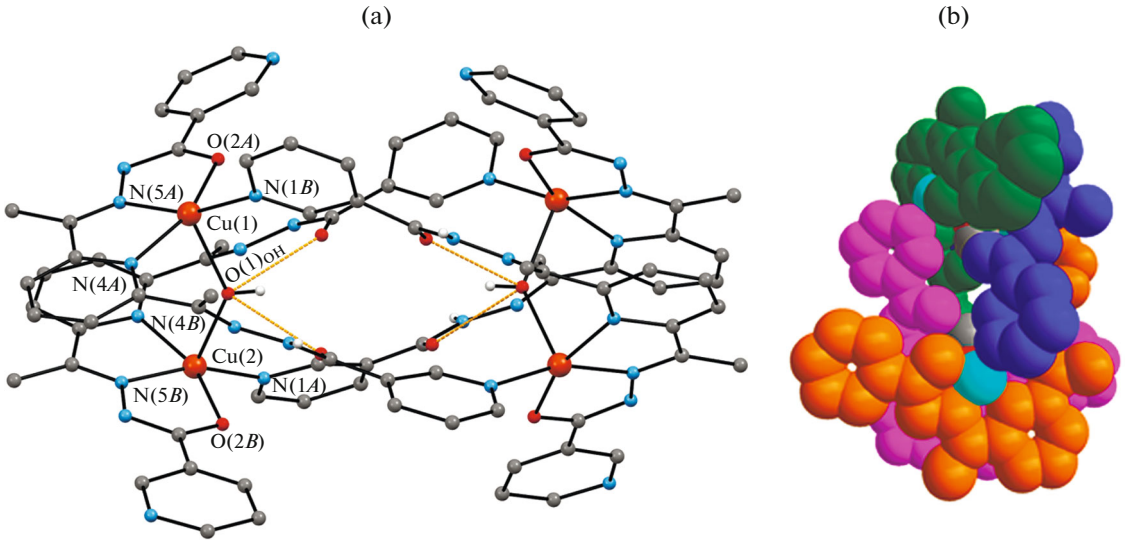

Fig. 5. Structures of the (a) tetranuclear complex cation $[Cu_4(HL^2)_4(OH)_2]^{2+}$ with the partial notation of atoms and (b) quaternary spiral for the tetranuclear complex cation $[Cu_4(HL^2)_4(OH)_2]^{2+}$.

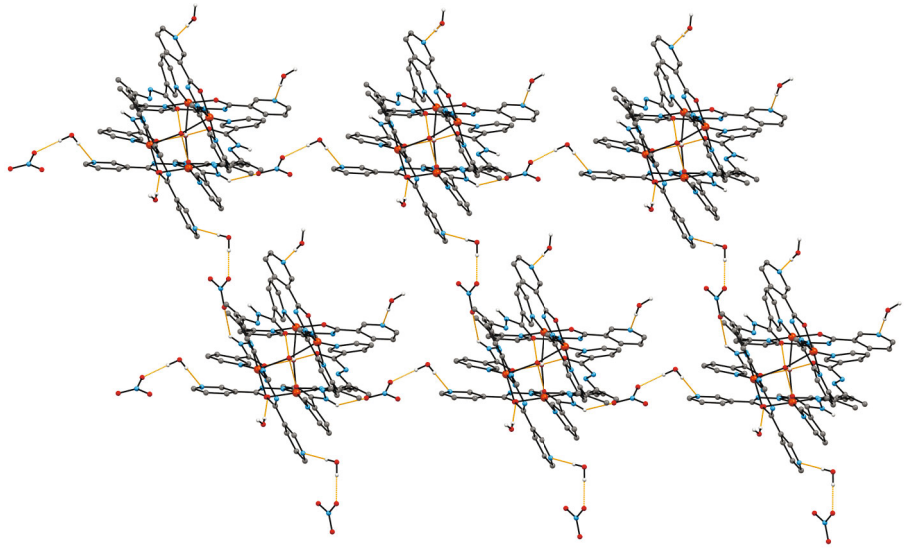

Fig. 6. Fragment of the crystal structure of compound **VI**.

was mentioned for the binuclear nickel(II) complex only [22].

The data of measurements of the magnetic susceptibility (χ_M) for the binuclear coordination compound $[Cu_2(H_2L^1)_2](SO_4)_2 \cdot 4H_2O$ were obtained for the polycrystalline product in the magnetic field with an induction of 0.1 T in a range of 300–2 K, whereas the magnetization isotherms were measured at 2 K in the range with an induction of 0–5 T (Fig. 7).

All data were corrected with allowance for the holder of the sample and Pascal's constants. The magnetic interaction constants and factors g_{Cu} were determined by the examination of the dependences $\chi_M T(T)$ and $\chi_M(T)$. The examination was performed taking into account the temperature-independent paramagnetism (TIP), contribution of paramagnetic impurities (ρ), and intermolecular interactions (zJ) via the equation

$$\chi_M(T) = \frac{\chi_d(T)}{\left[1 - 2zJ'\chi_d(T)/Ng^2\beta^2\right]}(1-\rho) + \rho\frac{Ng^2\beta^2}{3kT}S(S+1) + TIP.$$

The temperature dependence of the magnetic susceptibility for compound **I** is shown in Fig. 7. At 300 K the product $\chi_M T$ takes the value 0.94 cm^3 K mol^{-1}, which is well consistent with the theoretical value for two Cu(II) atoms (d^9, $S = 1/2$) with $g = 2.24$. As the temperature decreases, $\chi_M T$ increases continuously reaching a maximum value of 1.107 cm^3 K mol^{-1} at 4 K. This behavior indicates the ferromagnetic interaction between two paramagnetic centers. The sharp decrease in $\chi_M T$ after 4 K is explained by the intermolecular interaction between the binuclear complexes in the solid state.

Using the results of the structural study, the magnetic behavior of coordination compound **I** can be modeled on the basis of the isotropic Hamiltonian, which describes the interaction between two spins, $S_1 = S_2 = 1/2$,

$$H = -2JS_1S_2.$$

The theoretical values of magnetic susceptibility can be determined by the following analytical solution presented by the equation:

$$\chi_d = \frac{2Ng_{Cu}^2\beta^2}{Tk_B}\frac{1}{3+e^{-2J/k_BT}}.$$

The best coincidence of the theoretical and experimental values ($R = 1.57 \times 10^{-6}$) was obtained for the following set of variable parameters: $J = 3.38(6)$ cm^{-1}, $g = 2.251(2)$, $zJ' = -0.243(3)$ cm^{-1}, and TIP $= -6.49 \times 10^{-5}$ cm^3 K mol^{-1}, where zJ' is the contribution of the intermolecular interaction calculated from the magnetic susceptibility [26–28].

$$\chi(T) = \frac{\chi_d(T)}{\left[1-\frac{2zJ'\chi_d(T)}{Ng^2\beta^2}\right]}.$$

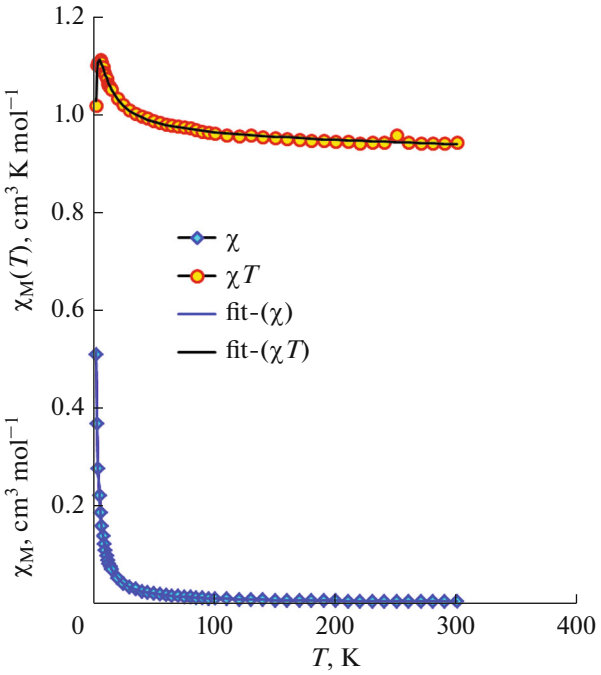

Fig. 7. Temperature dependences of $\chi_M T$ and χ_M for compound **I**.

The contribution of paramagnetic impurities is very low and was ignored in order to decrease the number of variable parameters.

The measurements of the magnetic susceptibility with inductions of 0.1 and 1.0 T at various temperatures and the measurements based on the magnetic fields for tetranuclear compound **VI** indicate the absence of a magnetic interaction (or an insignificant interaction) between the copper(II) ions (Fig. 8). A slight decrease in $\chi_M T(T)$ is observed after 4 K, which is probably the result of the intermolecular interaction.

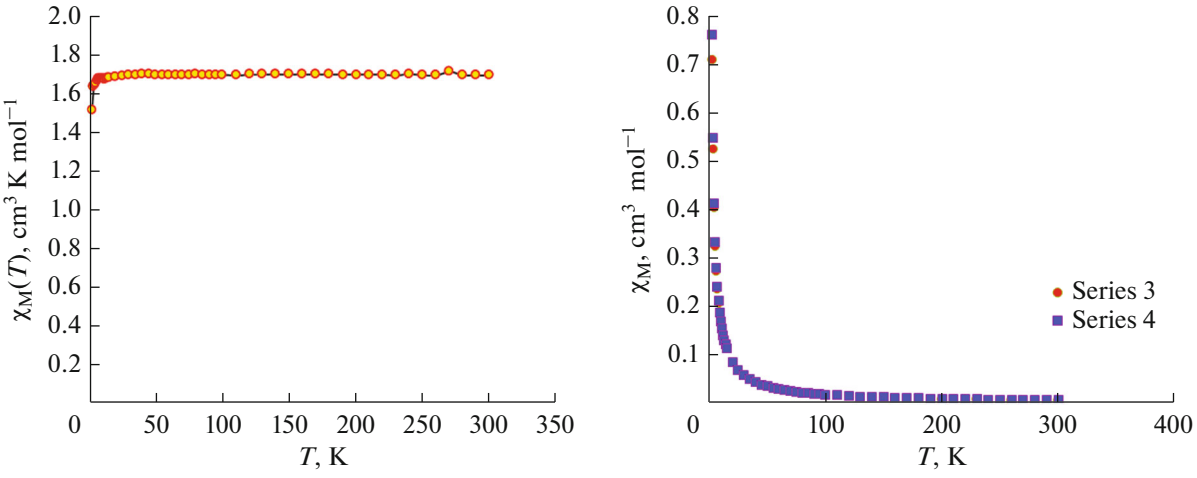

Fig. 8. Temperature dependences of $\chi_M T$ and χ_M for compound **VI**.

The indicated experimental value equal to 1.70 cm^3 K mol^{-1} at 300 K corresponds to four Cu(II) ions with $g = 2.13$. The absence of a magnetic interaction is consistent with long distances between the copper(II) atoms (Cu(1)···Cu(2) 4.298 Å) and the presence of the OH^- bridge joining two copper(II) ions along the coordinate 5 of the coordination polyhedron (tetragonal pyramid) at a relatively long distance (Fig. 8).

According to the temperature dependence of the magnetic susceptibility (2–300 K), the copper(II) ions with $S = 1/2$ interact weakly with each other ($2J = -0.05(1)$ cm^{-1}, $g = 2.15(2)$). The weak magnetic interaction for the Cu_4 cluster was confirmed by measurements of the magnetic susceptibility in the fields of various inductions (0–5 T), which is explained by longer bonds between the Cu(1) and Cu(2) copper ions and the O(1) oxygen atom of the bridging groups OH^-.

REFERENCES

1. Bottari, B., Maccari, R., Monforte, F., et al., *Bioorg. Med. Chem.*, 2001, vol. 9, p. 2203.
2. Carcelli, M., Ianelli, S., Pelagatti, P., and Pelizzi, G., *Inorg. Chim. Acta*, 1999, vol. 292, p. 121.
3. Neto, B.A.D., Viana, B.F.L., Rodrigues, T.S., et al., *Dalton Trans.*, 2013, vol. 42, p. 11497.
4. Panja, A., Campana, C., Leavitt, C., et al., *Inorg. Chim. Acta*, 2009, vol. 362, p. 1348.
5. Naskar, S., Mishra, D., Blake, A.J., and Chattopadhyay, Sh.K., *Struct. Chem.*, 2007, vol. 18, no. 2, p. 217.
6. Naskar, S., Mishra, D., Chattopadhyay, Sh.K., Corbella, M., et al., *Dalton Trans.*, 2005, vol. 14, p. 2428.
7. Naskar, S., Corbella, M., Blake, A.J., and Chattopadhyay, Sh.K., *Dalton Trans.*, 2007, vol. 11, p. 1150.
8. Bulhac, I., Deseatnic-Ciloci, A., Bourosh, P., et al., *Chem. J. Mold.*, 2016, vol. 11, p. 39.
9. Bourosh, P., Bulhac, I., Mirzac, A., et al., *Russ. J. Coord. Chem.*, 2016, vol. 42, p. 157. https://doi.org/10.1134/S1070328416030015
10. Bulhac, I., Danilescu, O., Rija, A., et al., *Russ. J. Coord. Chem.*, 2017, vol. 43, p. 21. https://doi.org/10.1134/S1070328417010018
11. Mazza, P., Orcesi, M., Pelizzi, C., et al., *J. Inorg. Biochem.*, 1992, vol. 48, p. 251.
12. Koziol, A.E., Palenik, R.C., Palenik, G.J., and Wester, D.W., *Inorg. Chim. Acta*, 2006, vol. 359, p. 2569.
13. *CrysAlis RED, O.D.L. Version 1.171.34.76*, 2003.
14. Sheldrick, G., *Acta Crystallogr., Sect. A: Found. Crystallogr.*, 2008, vol. 64, no. 1, p. 112.
15. Bellamy, L.J., *The Infrared Spectra of Complex Molecules*, New York: Wiley, 1958.
16. Tarasevich, B.N. *IK spektry osnovnykh klassov organicheskikh soedinenii. Spravochnye materialy* (IR Spectra of Main Classes of Organic Compounds. Reference Materials), Moscow, 2012.
17. Nakanishi, K., *Infrared Absorption Spectroscopy*, Tokyo: Holden-Day, 1963.
18. Gordon, A. and Ford, R., *The Chemist's Companion: A Handbook of Practical Data, Techniques, and References*, New York: Wiley, 1972.
19. Nakamoto, K., *Infrared Spectra and Raman Spectra of Inorganic and Coordination Compounds*, New York: Wiley, 1986.
20. Yano, T., Tanaka, R., Nishioka, T., et al., *Chem. Commun.*, 2002, p. 1396.
21. Glatz, G. and Kempe, R., *Z. Kristallogr. NCS*, 2008, vol. 223, no. 3, p. 313.
22. Paolucci, G., Stelluto, S., Sitran, S., et al., *Inorg. Chim. Acta*, 1992, vol. 193, no. 1, p. 57.
23. Bino, A. and Cohen, N., *Inorg. Chim. Acta*, 1993, vol. 210, p. 11.
24. Bis, J.A. and Zaworotko, M.J., *Crystal Growth Des.*, 2005, vol. 5, no. 3, p. 1169.
25. Cowan, J.A., Howard, J.A.K., McIntyre, G.J., et al., *Acta Crystallogr., Sect. B: Struct. Sci.*, 2003, vol. 59, p. 794.
26. Kahn, O., *Molecular Magnetism*, New York: VCH, 1993.
27. O'Connor, C.J., *Prog. Inorg. Chem.*, 1982, vol. 29, p. 203.
28. Myers, B.E., Berger, L., and Friedber, S.A., *J. Appl. Phys.*, 1969, vol. 40, p. 1149.

Translated by E. Yablonskaya